Lecture 9: Polyelectrolyte Hydrogels

Last Day: Physical hydrogels
Structure and chemistry

Today: polyelectrolyte hydrogels, complexes, and coacervates
Polyelectrolyte multilayers
theory of swelling in ionic hydrogels

Reading: S.K. De et al., 'Equilibrium swelling and kinetics of pH-responsive hydrogels: Models, experiments, and simulations,' J. Microelectromech. Sys. 11(5) 544 (2002).

Supplementary Reading: L. Brannon-Peppas and N.A. Peppas, 'Equilibrium swelling behavior of pH-sensitive hydrogels,' *Chem. Eng. Sci*. **46**(3) 715-722 (1991).

USE DEMO OF AMINOETHYL METHACRYLATE HYDROGEL TO SHOW PH-DEPENDENT SWELLING?

Covalent polyelectrolyte hydrogels

Response of polyelectrolyte gels to pH of environment

- Reminder of the response of ionizable groups to pH changes:

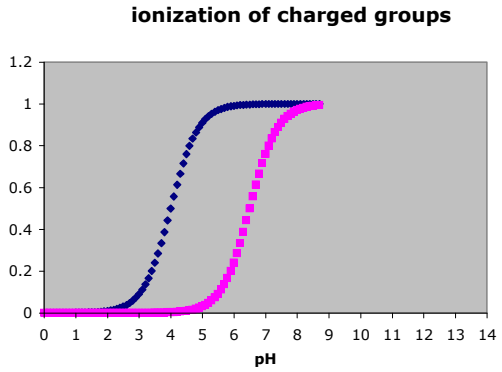

- Presence of ionizable groups makes polyelectrolyte hydrogels sensitive to:
  - pH
  - Ionic strength
  - Electric fields
  - (T)

- Observed swelling as a function of pH:
  - Data[1] for poly(2-hydroxyethyl methacrylate-co-acrylic acid) gels cross-linked with ethylene glycol dimethacrylate

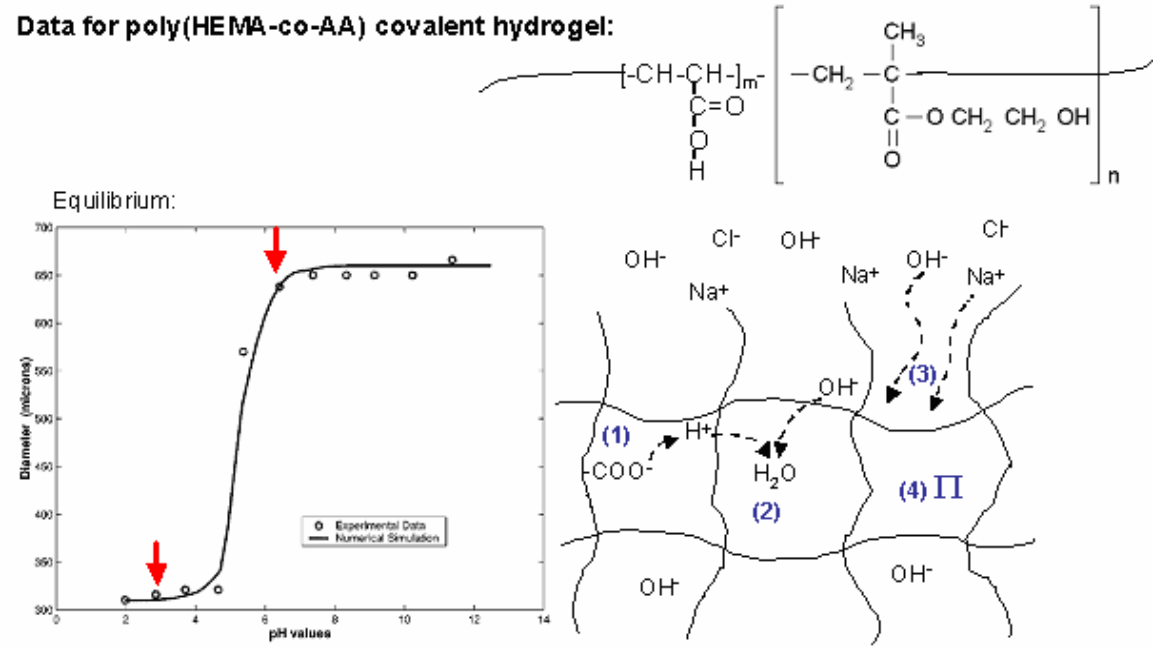

  - Physical chemistry of swelling at high pH (example for anionic gels):
    - Stepwise process in basic solutions:[1]
      1. Ionization of carboxyl groups, releasing H^+
         a. At high ionic group density, carboxylate anions repel one another, driving swelling- *but this is not the main driving force for swelling in typical conditions*
            i. Electrostatic force decays as $1/r^2$, too weak at typical charged group separation to have a significant effect
            ii. In water: $F = q_1q_2/4\pi\varepsilon r^2 = -e^2/4\tau\varepsilon r^2 = 2.04\times10^{-39}/r^2$ (r in m)
               1. $\varepsilon = 80$ in water
               2. $e = 1.602\times10^{-19}$ C
            iii. F1 nm/F0.2 nm = 0.04!
      2. H^+ recombines with OH^- to give water
      3. Charge is compensated by diffusion of cations (e.g. Na^+) and OH^- into gel
      4. Influx of new ions creates osmotic pressure that drives swelling[2]

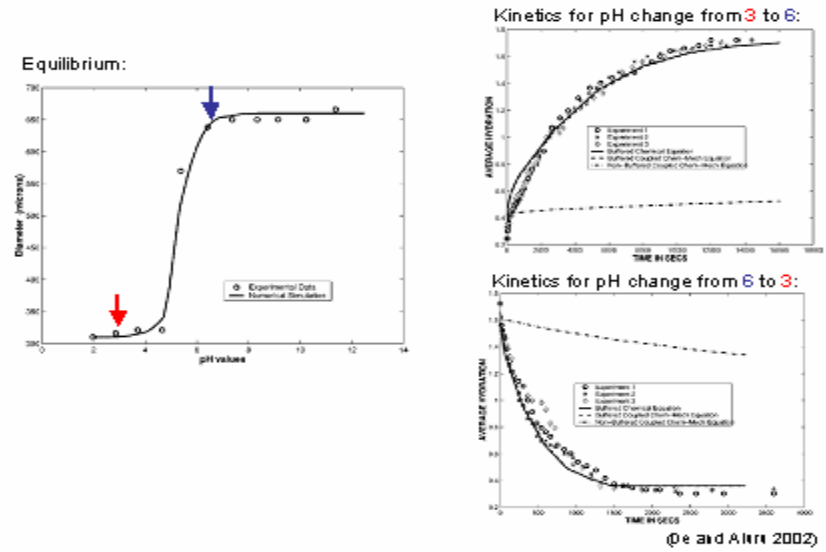

- Kinetics: deswelling faster (~10X) than swelling
  - Swelling in ~166 min.
  - De-swelling in ~16 min.
  - (300 μm thick gels)
  - Theory based on diffusion of ions into and out of gel semi-quantitatively predicts observed swelling behavior
    - Implies that response time of gels will scale *inversely* with the *size* of the gel
    - Swelling rate inversely proportional to square of gel size^3
    - Swelling rate can also be increased by creating greater porosity in gel- increase surface/volume ratio allows solute to diffuse into gel more rapidly

Rapid swelling/deswelling of superporous gels:

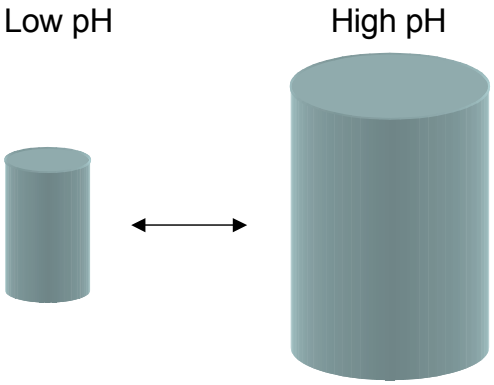

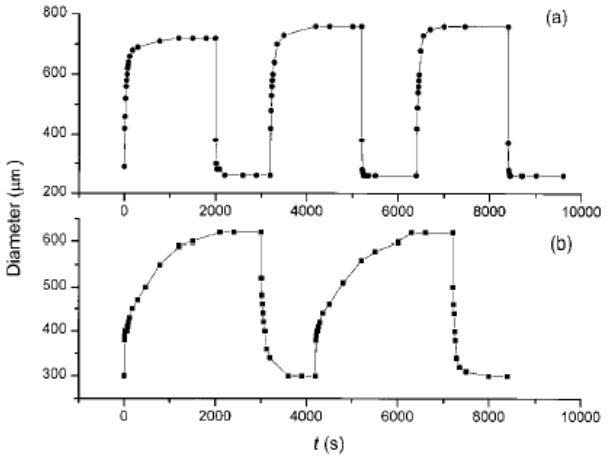

Figure 2. Swelling and shrinking kinetics of hydrogels **1** (a) and **2** (b) in a pH = 11.77 NaOH solution and a pH = 1.92 buffer solution with ionic strength of 0.2 M. Three cycles of swelling and shrinking were shown for gel **1**; two cycles were shown for gel **2**.

(Zhao and Moore, 2001)

- hydrogels containing basic groups show opposite pH sensitivity
  - swelling in acidic solutions
  - e.g. Peppas papers

Polyion complex hydrogels[4]

Coacervates

- complexation between two oppositely charged polyelectrolytes can lead to:
  1. precipitation (insoluble solid phase)
     - driven by charge neutralization on hydrophobic polymers
     - driven by macro-aggregate formation
  2. coacervate formation (dense liquid phase)
  3. soluble complexes

- mechanisms of formation

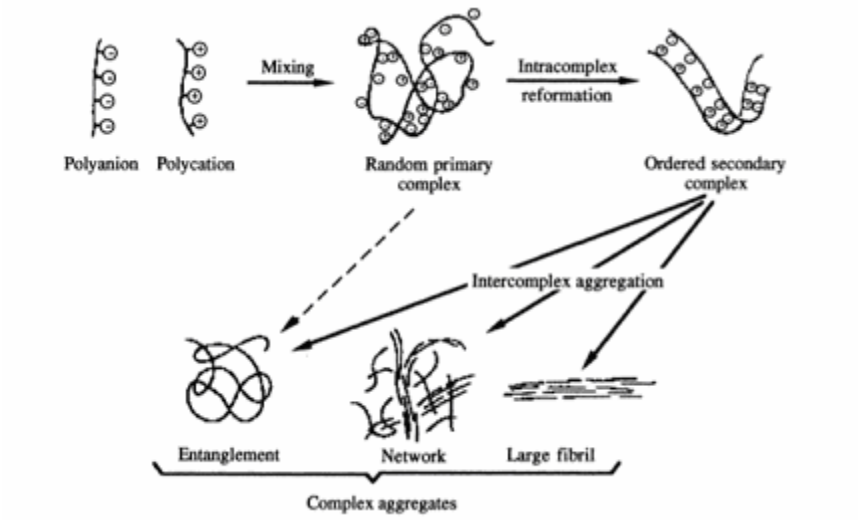

  1. initial rapid Coulombic bonding
  2. formation of new bonds/restructuring of chain distortions
  3. aggregation of secondary complexes
  - mixing of two polyions can lead to 90% complex formation

- Polyelectrolytes studied as coacervates for biomaterials:[4]
  - Polyanions
    - Carboxymethylcellulose
    - Alginate
    - Dextran sulfate
    - Carboxymethyl dextran
    - Heparin
    - Carrageenan
    - Pectin
    - xanthan
  - Polycations
    - Chitosan (derived from crab shells)
    - Polyethyleneimine
    - Poly(4-vinyl-N-butylpyridinium) bromide
    - Quarternized polycations
    - Poly(vinylbenzyltrimethyl)ammonium hydroxide

- Microstructure of coacervate hydrogels
  - Example structures: xanthan/chitosan coacervates (Dumitriu et al. 1998)

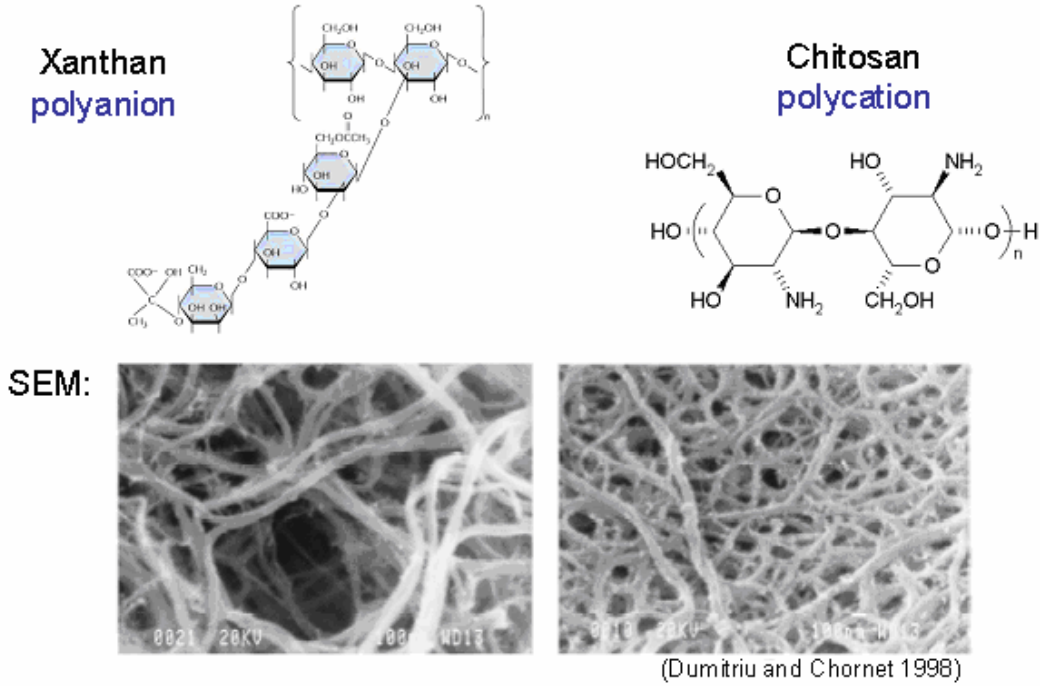

(Dumitriu and Chornet 1998)

  - Pore sizes formed 0.1-1 μm; fiber diameters ~100 nm

Polyelectrolyte multilayers (PEMs)

Structure of PEMs

Assembly

- Layer-by-layer deposition
  - How is it done
  - Surface properties change in digital fashion with adsorption of sequential layers[5]

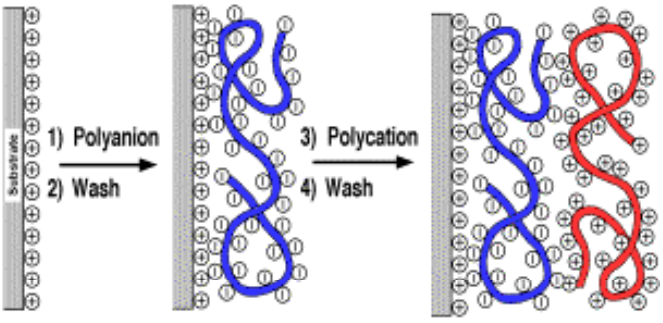

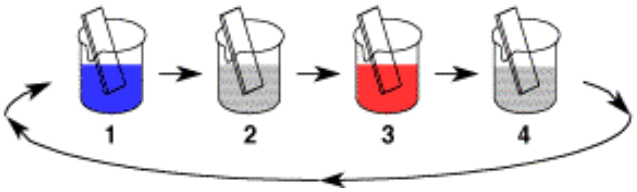

Surface properties dominated by last layer deposited:

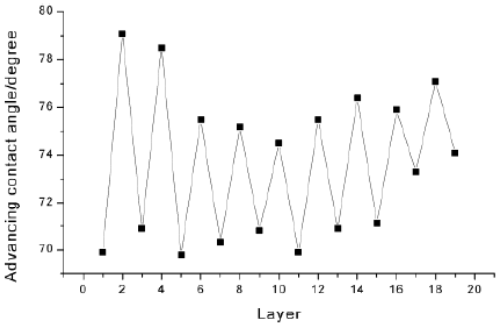

Figure 2. Advancing contact angle as a function of the layer number of PSS and chitosan. Odd numbers represent films with PSS as the outermost layer, whereas even number films have chitosan as the outermost layer.

- Assembly figure source: http://www.chem.fsu.edu/multilayers/

- Assembly on complex surfaces
  - Polyelectrolytes will adsorb to surfaces with complex topography
  - Polyelectrolytes themselves may have complex geometries (e.g. particles or dendrimers)[6]

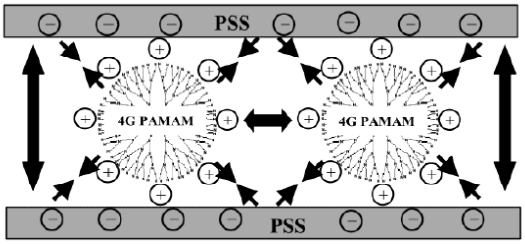

Generation 7 poly(amidoamine) dendrimer:

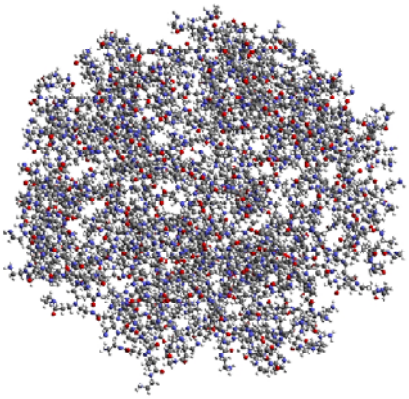

Scheme 1. Schematic Illustration for the Preparation of Hollow PSS/4G PAMAM Multilayer Capsules

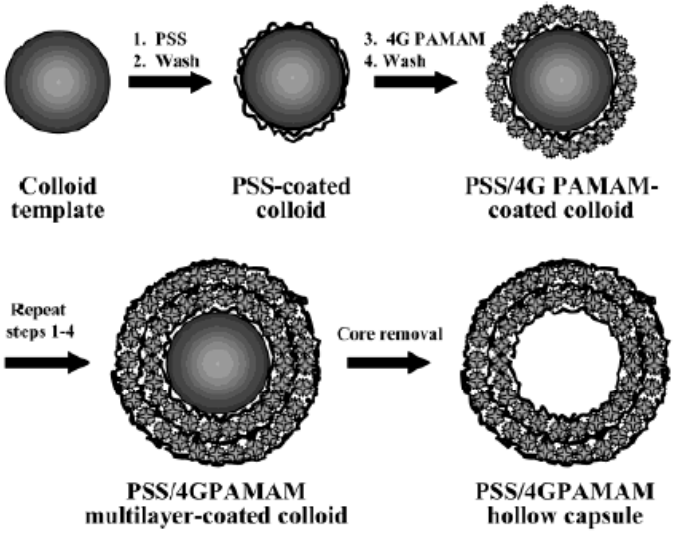

(Khopade and Caruso, 2002)

- Dendrimer image source: http://www.foresight.org/Conferences/MNT7/Papers/Cagin3/

- Assembly on protein crystals to encapsulate proteins:[7]
  - Blah blah

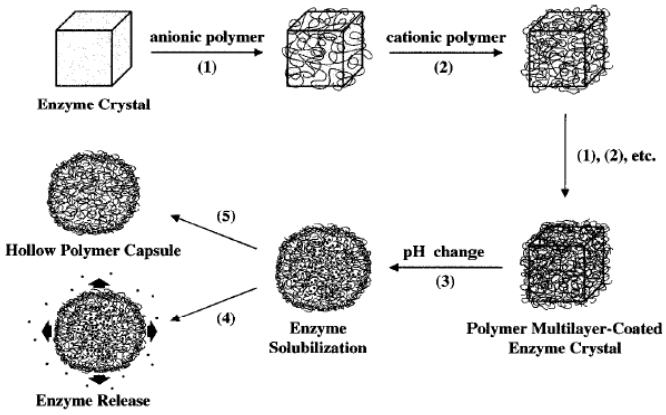

Figure 1. Scheme showing the process used to encapsulate enzymes by using biocrystals as templates for the deposition of polymer multilayers, subsequent enzyme solubilization and release, and the formation of hollow polymer capsules. (1, 2) Polyelectrolyte layers are deposited stepwise onto the crystals by making use of the surface charge reversal that occurs upon adsorption of each layer. Each polyelectrolyte layer deposited bears an opposite charge to that already adsorbed. Excess, unadsorbed polyelectrolyte is removed by repeated centrifugation/wash redispersion cycles before the next layer is deposited. (3) Solubilization of the enzyme inside the polymer capsule by exposure to solutions of pH > 6 or acidic solution (pH < 4) results in a morphology change of the polymer capsule. (4) Release of the enzyme by rupturing the polymer capsule, achieved by exposure to solutions of pH > 11. (5) Exposure of the encapsulated enzyme to an oxidizing solution results in decomposition of the enzyme which then is expelled from the interior through the polymer walls, leaving behind hollow polymer capsules that originally encapsulate the enzyme.

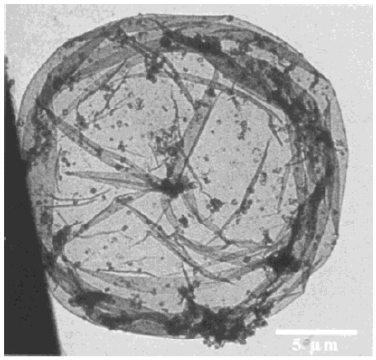

Figure 4. TEM image of an air-dried hollow polymer capsule comprising eight $[(PSS/PAH)_4]$ polyelectrolyte layers, obtained after decomposition of the encapsulated enzyme. The polymer capsule spreads out on the carbon surface on which it is dried, and folds and creases can be seen. Some undecomposed enzyme can still be seen in the interior of the capsule.

(Caruso et al., 2000)

- Cells as living PEM assembly substrates:

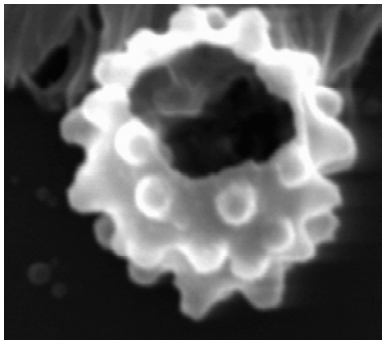

SEM micrograph of multilayer-coated echinocyte blood cell (F. Caruso)

(Source: http://www.chem.fsu.edu/multilayers/)

- What else

Building PEMs on biomaterials[8]

- Assembly of PEMs on amino-modified poly(lactide)[5]
  - Alternating adsorption of sulfonated polystyrene and chitosan (polycation)

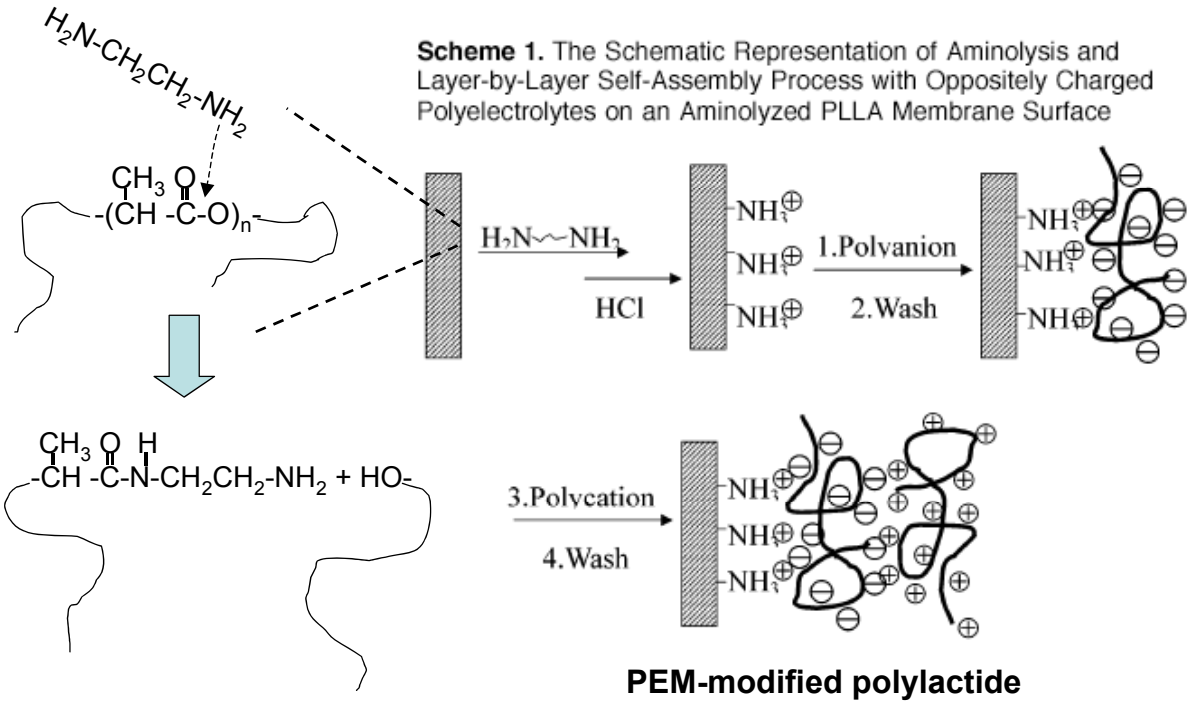

Scheme 1. The Schematic Representation of Aminolysis and Layer-by-Layer Self-Assembly Process with Oppositely Charged Polyelectrolytes on an Aminolyzed PLLA Membrane Surface

PEM-modified polylactide

Utility of polyeletrolyte gels in biomaterials/bioengineering

- **Cell encapsulation**: *In situ* formation with no 'additives', no change in pH, no change in temperature, in physiological solutions
  - Useful for safe encapsulation of cells
- **Drug delivery**: Ionic interactions for protein-polymer complexes prior to gel formation allow high protein entrapment efficiencies
  - PEMs can form hollow capsules

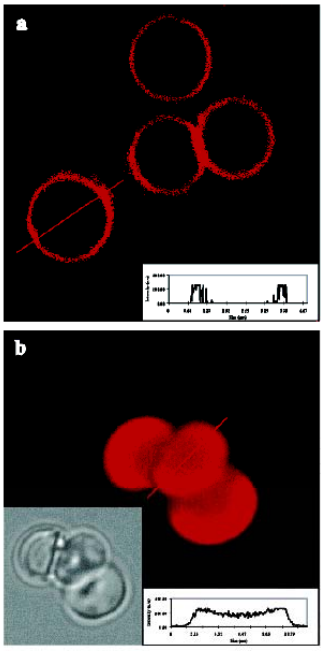

Fluorescent drug-loaded PEM capsules

Drug release from PSS/PAMAM PEM capsules:

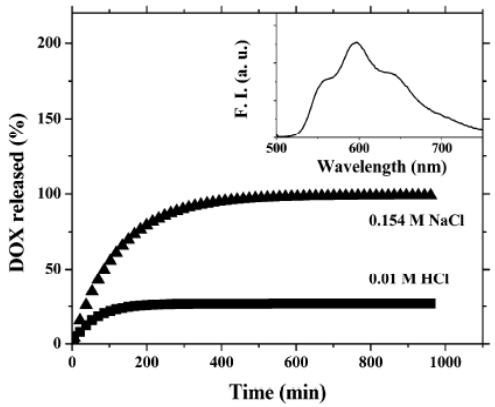

Figure 4. Release profiles for encapsulated DOX in PSS/4G PAMAM capsules in 0.01 M HCl and 0.154 M NaCl solutions. The capsules were stabilized with DOX and preloaded with DS prior to encapsulation of the DOX in their interior. The inset shows a fluorescence spectrum of a DOX-loaded PSS/4G PAMAM capsule suspension that was used for release studies. The excitation wavelength was 480 nm.

- **Enzyme immobilization**: binding to ionic groups for biosensors or active biomaterials
- **Protein separations/recovery**:[9] some binding specificity can be achieved in certain situations to allow for selective sorption of a target protein
  - Addition of polycation or polyanion to solution of protein leads to protein-polyelectrolyte coacervate formation
  - Bound proteins released by adjustment of pH/ionic strength

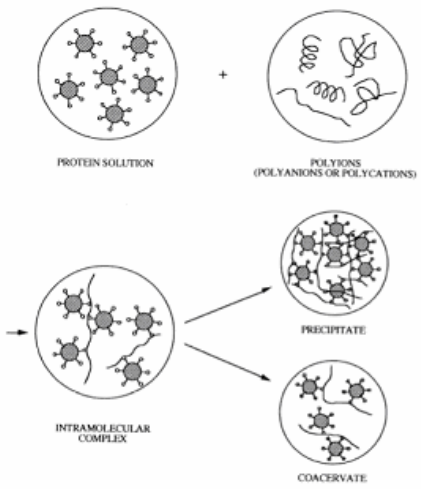

Fig. 6. The mechanism of protein–polyelectrolyte complexes formation.

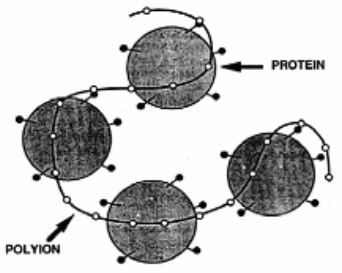

Fig. 21. Structure of an intramolecular complex. The open and solid circles represent ionizable groups in the polyion and protein, respectively. From Ref. [157].

- **Microvalves for bioMEMS and lab-on-a-chip applications**:[10,11] Utilize fast response of swelling in microsized gels to control flow through microfluidics
  - **Example**: PHEMA-co-AA networks patterned in microfluidic channels:

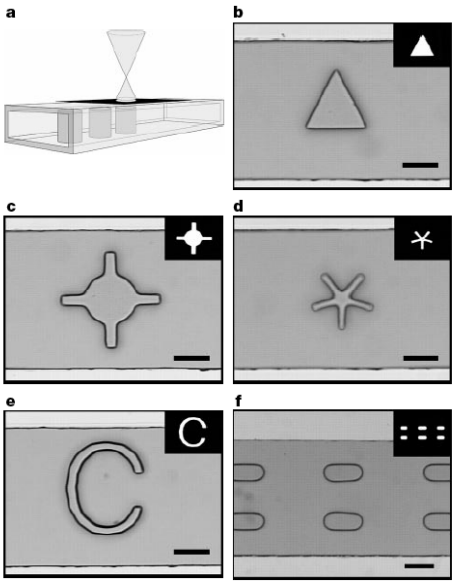

Figure 1 A diagram of the fabrication method and images demonstrating a variety of shapes that were polymerized within 35 seconds. **a**, The fabrication method. **b**, A polymerized hydrogel demonstrating the ability to pattern high-definition straight edges. The corresponding photomask is shown at a reduced size in the upper right corner of each picture. **c**, **d**, Structures illustrating the generation of convex and concave surfaces. **e**, A structure with high-aspect-ratio features. Imperfections in the mask were transferred to the structure, further demonstrating the high fidelity of the photolithographic process. **f**, The simultaneous polymerization of multiple structures with a single exposure of ultraviolet light. Scale bars: **b**–**e**, 250 μm; **f**, 500 μm.

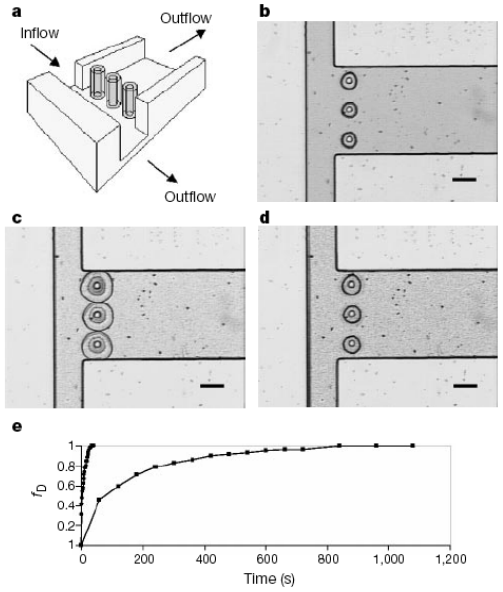

Figure 2 Prefabricated posts in a microchannel serve as supports for the hydrogels, improving stability during volume changes. **a**, A diagram of the hydrogel jackets around the posts. **b**, The actual device after polymerization of the hydrogel. **c**, The hydrogel jackets block the side channel branch in their expanded state. **d**, The contracted hydrogels allow fluid to flow down the side branch. **e**, The improvement in time response of the hydrogel jacket design (circles) versus an alternative design that uses a single larger cylindrical structure in the same size channel (squares). f_D is the fractional change in diameter. Scale bars, 300 μm.

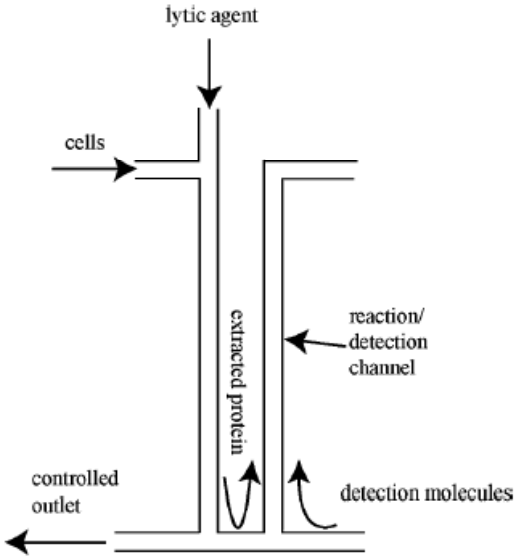

Figure 12 Lytic agent diffuses into the cell stream, lysing the cells and releasing the protein of interest. A small volume of the proteins are routed into the detection channel where molecules from a stream of detection reagent diffuse into the proteins, giving off a fluorescent signal.

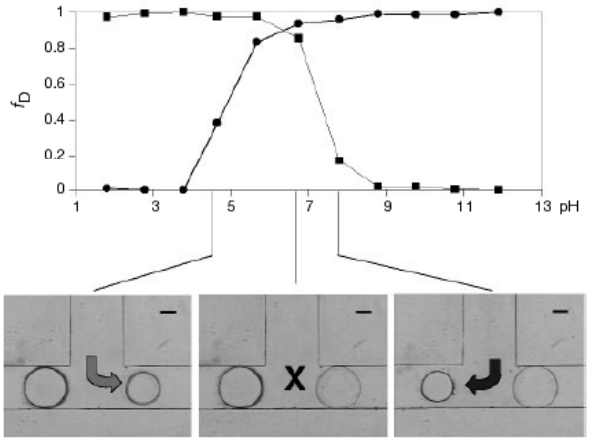

Figure 4 The volume response of two different hydrogels with respect to the pH of the surrounding fluid. Top, the fractional change in diameter (f_D) of the hydrogels with respect to pH. Bottom, images showing a device that directs ('sorts') a fluid stream on the basis of its pH. The hydrogel gating the right branch (circles) expands in base and contracts in acid. The hydrogel gating the left branch (squares) behaves in the opposite manner (expands in acid and contracts in base). The fluid enters from the centre channel at a rate of 0.05 ml min^{-1}. At a pH of 7.8, the flow is directed down the left branch. At a pH of 4.7, the flow is directed down the right branch. Both hydrogels expand to shut off the flow when the pH is changed to 6.7. Scale bars, 300 μm.

- Schematic shows an example lab-on-a-chip analysis approach

  - Second figure on right depicts a sorting valve that can determine whether fluid flow goes left or right based on pH of solution
    - Composed of one polybase gel (poly(dimethylaminoethyl methacrylate-co-hydroxyethyl methacrylate) cross-linked by ethylene glycol dimethacrylate and other gel poly(acrylic acid-co-hydroxyethyl methacrylate)
    - Base gel swells at low pH, acid gel swells at high pH

- **Surface modification agents**: as described above for polylactide and other biomaterials

Brannon-Peppas theory of swelling in ionic hydrogels

- Original theory for elastic networks developed by Flory and Mehrer[12-14], refined for treatment of ionic hydrogels by Brannon-Peppas and Peppas[15,16]
- Other theoretical treatments[17]

Derivation of ionic hydrogel swelling

- Model structure of the system:

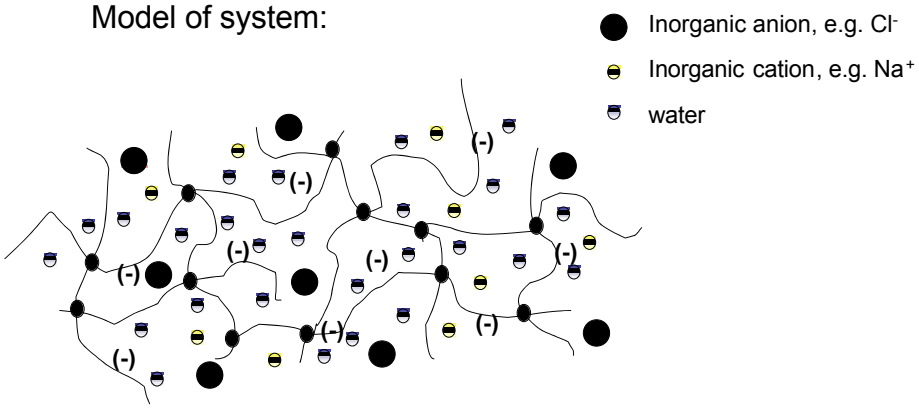

- System is composed of permanently cross-linked polymer chains, water, and salt
- We will derive the thermodynamic behavior of the ionic hydrogel using the model we previously developed for neutral hydrogels swelling in good solvent

- Model parameters:

a_+	activity of cations in gel
a_+^*	activity of cations in solution
a_-	activity of anions in gel
a_-^*	activity of anions in solution
c_+	concentration of cations in gel (moles/volume)
c_+^*	concentration of cations in solution (moles/volume)
c_-	concentration of anions in solution (moles/volume)
c_-^*	concentration of anions in solution (moles/volume)
c_s	concentration of electrolyte
c_2	concentration of ionizable repeat units in gel (moles/volume)
μ_1^*	chemical potential of water in solution
μ_1	chemical potential of water in the hydrogel
μ_1^0	chemical potential of pure water in standard state
M	Molecular weight of polymer chains before cross-linking
M_c	Molecular weight of cross-linked subchains
n_1	number of water molecules in swollen gel
χ	polymer-solvent interaction parameter

k_B	Boltzman constant
T	absolute temperature (Kelvin)
$v_{m,1}$	molar volume of solvent (water, volume/mole)
$v_{m,2}$	molar volume of polymer (volume/mole)
$v_{sp,1}$	specific volume of solvent (water, volume/mass)
$v_{sp,2}$	specific volume of polymer (volume/mass)
V_2	total volume of polymer
V_s	total volume of swollen hydrogel
V_r	total volume of relaxed hydrogel
ν	number of subchains in network
ν_e	number of 'effective' subchains in network
ν^+	stoichiometric coefficient for eletrolyte cation
ν^-	stoichiometric coefficient for eletrolyte anion
$\phi_{1,s}$	volume fraction of water in swollen gel
$\phi_{2,s}$	volume fraction of polymer in swollen gel
$\phi_{2,r}$	volume fraction of polymer in relaxed gel
x_1	mole fraction of water in swollen gel
x_1^*	mole fraction of water in solution

- Asterisks denote parameters in solution

- Free energy has 3 components: free energy of mixing, elastic free energy, and ionic free energy

Eqn 1 $\Delta G_{total} = \Delta G_{mix} + \Delta G_{el} + \Delta G_{ion}$

- At equilibrium, the chemical potential of water inside and outside the gel are equal:

Eqn 2 $\mu_1^* = \mu_1$

Eqn 3 $\mu_1^* - \mu_1^0 = \mu_1 - \mu_1^0$

  - Solution contains ions so μ_1^* is not equal to μ_1^0

Eqn 4 $(\Delta\mu_1^*)_{TOTAL} = (\Delta\mu_1)_{TOTAL}$

Eqn 5 $(\Delta\mu_1^*)_{ion} = (\Delta\mu_1)_{mix} + (\Delta\mu_1)_{el} + (\Delta\mu_1)_{ion}$

  - The equation we'll try to solve is a rearrangement of this:

Eqn 6 $(\Delta\mu_1^*)_{ion} - (\Delta\mu_1)_{ion} = (\Delta\mu_1)_{mix} + (\Delta\mu_1)_{el}$

- Contributions to the free energy:
  - Free energy of mixing:

Eqn 7 $\Delta G_{mix} = \Delta H_{mix} - T\Delta S_{mix}$

  - We previously derived the contribution from mixing using the Flory-Rehner lattice model:

Eqn 8 $\Delta G_{mix} = k_B T[n_1 \ln(1-\phi_{2,s}) + \chi n_1 \phi_{2,s}]$

Eqn 9 $$(\Delta\mu_1)_{mix} = \left(\frac{\partial(\Delta G_{mix})}{\partial n_1}\right)_{T,P} = k_B T[\ln(1-\phi_{2,s}) + \phi_{2,s} + \chi\phi_{2,s}^2] = RT[\ln(1-\phi_{2,s}) + \phi_{2,s} + \chi\phi_{2,s}^2]$$

    - Second expression puts us on a molar basis instead of per molecule

  - Elastic free energy:

Eqn 10 $\Delta G_{el} = (3/2)k_B T\nu_e(\alpha^2 - 1 - \ln\alpha)$

Eqn 11
$$(\Delta\mu_1)_{el} = \left(\frac{\partial(\Delta G_{el})}{\partial n_1}\right)_{T,P} = \left(\frac{\partial(\Delta G_{el})}{\partial\alpha}\right)_{T,P}\left(\frac{\partial\alpha}{\partial n_1}\right)_{T,P} = RT\nu\left(1-\frac{2M_c}{M}\right)\frac{v_{m,1}}{V_r}\left[\left(\frac{\phi_{2,s}}{\phi_{2rs}}\right)^{1/3} - \frac{1}{2}\left(\frac{\phi_{2,s}}{\phi_{2rs}}\right)\right]$$

$$= RT\left(\frac{v_{m,1}}{v_{sp,2}M_c}\right)\left(1-\frac{2M_c}{M}\right)\phi_{2,r}\left[\left(\frac{\phi_{2,s}}{\phi_{2rs}}\right)^{1/3} - \frac{1}{2}\left(\frac{\phi_{2,s}}{\phi_{2rs}}\right)\right]$$

- Last equality uses:
  - $\nu = V_2/v_{sp,2}M_c$ (on handout)
  - $V_r = V_2/\phi_{2,r}$ (on handout)
  - Thus $\nu/V_r = \phi_{2,r}/v_{sp,2}M_c$

  - Ionic free energy:
    - Term driving dilution of ions diffusing into gel to maintain charge neutrality

- Chemical potential change in solution:

Eqn 12 $$(\Delta\mu_1)^*_{ion} = \mu_1^* - \mu_1^0 = RT\ln a_1^* \cong RT\ln x_1^* = RT\ln(1 - \sum_j^{all\_solutes} x_j^*)$$

- approximation in third equality is used for dilute solutions

Eqn 13 $$(\Delta\mu_1)^*_{ion} \cong -RT\sum_j^{all\_ions} x_j^* = -\frac{RT}{n}\sum_j^{all\_ions} n_j^* = -\frac{v_{m,1}RT}{v_{m,1}n}\sum_j^{all\_ions} n_j^* \cong -v_{m,1}RT\sum_j^{all\_ions} c_j^*$$

- The first approximation holds if Σx_j^* is small
- Fourth equality holds because we assume in the liquid lattice model that the molar volume of all species is the same, thus $v_{m,1}n = V$, the total volume of the system

- Chemical potential change in gel:

Eqn 14 $$(\Delta\mu_1)_{ion} = \mu_1 - \mu_1^0 = RT\ln a_1 \cong -v_{m,1}RT\sum_j^{all-ions} c_j$$

Eqn 15 $$(\Delta\mu_1)^*_{ion} - (\Delta\mu_1)_{ion} = -v_{m,1}RT\sum_j^{all-ions}(c_j - c_j^*)$$

- The electrolyte dissolved in water provides mobile cations and anions in the solution and in the gel:
  - E.g. NaCl: $Na^+{}_{\nu+}Cl^-{}_{\nu+\,(s)} \rightarrow \nu^+Na^+_{(aq)} + \nu^-Cl^-_{(aq)}$
  - $\nu^+ = \nu^- = 1$ stoichiometric coefficients

Eqn 16 $$C^{z+}_{\nu_+}A^{z-}_{\nu_-} \rightarrow \nu_+C^{z+} + \nu_-A^{z-}$$

- e.g. $CaCl_2$: $\nu_+ = 1$, $\nu_- = 2$, $z_+ = 2$, $z_- = 1$

Eqn 17 $$\nu^+ + \nu^- = \hat{\nu}$$ **…for a 1:1 electrolyte**

Eqn 18 $$\nu^+ = \nu^- = \frac{\hat{\nu}}{2}$$ **…for a 1:1 electrolyte**

Eqn 19 $$c_+^* + c_-^* = (\nu^+ + \nu^-)c_s^* = \hat{\nu}c_s^*$$ **…total concentration of ions**

- We will derive equations for an anionic network
  - Assuming activities ~ concentrations
  - Inside gel:

Eqn 20 $c_+ = \nu_+c_s$

Eqn 21 $c_- = \nu_-c_s + ic_2/z_-$

- c_2 is the moles of ionizable repeat groups on gel chains per volume
- First term comes from electrolyte anions in gel, second term from counter-ions associated with ionized groups on the polymer chains
- The degree of ionization *i* can be related to the pH of the environment and the pKa of the network groups:

Eqn 22 $$K_a = \frac{[RCOO^-][H^+]}{[RCOOH]}$$

Eqn 23

$$i = \frac{[RCOO^-]}{[RCOOH]+[RCOO^-]} = \frac{\frac{[RCOO^-]}{[RCOOH]}}{1+\frac{[RCOO^-]}{[RCOOH]}} = \frac{\frac{K_a}{[H^+]}}{1+\frac{K_a}{[H^+]}} = \frac{K_a}{[H^+]+K_a} = \frac{K_a}{10^{-pH}+K_a} = \frac{10^{-pK_a}}{10^{-pH}+10^{-pK_a}}$$

- Outside gel:

Eqn 24 $c_+^* = \nu_+ c_s^*$

Eqn 25 $c_-^* = \nu_- c_s^*$

- Our relationship for the ionic chemical potentials is now:

Eqn 26
$$(\Delta\mu_1)_{ion}^* - (\Delta\mu_1)_{ion} = \nu_{m,1}RT\sum_j^{all-ions}(c_j - c_j^*) = \nu_{m,1}RT(c_+ + c_- - c_+^* - c_-^*)$$

- Using Eqn 20, Eqn 21, Eqn 24, and Eqn 25, Eqn 26 becomes:

Eqn 27
$$(\Delta\mu_1)_{ion}^* - (\Delta\mu_1)_{ion} = \nu_{m,1}RT\left(\nu_+ c_s + \nu_- c_- + \frac{ic_2}{z_-} - \hat{\nu}c_s^*\right) = \nu_{m,1}RT\left(\hat{\nu}\, c_s + \frac{ic_2}{z_-} - \hat{\nu}c_s^*\right)$$

$$= \nu_{m,1}RT\left(\frac{ic_2}{z_-} - \hat{\nu}(c_s - c_s^*)\right)$$

- **How can we relate c_s and c_s^*?**
  - We can make simplifications for a 1:1 cation:anion electrolyte:
  - The chemical potentials of the mobile ions must also be equilibrated inside/outside the gel:

Eqn 28 $\mu_+ = \mu_+^*$

Eqn 29 $\mu_- = \mu_-^*$

- Add Eqn 29 to Eqn 28:

Eqn 30 $\mu_+ + \mu_- = \mu_+^* + \mu_-^*$

Eqn 31
$$RT\ln a_+^{\nu_+} + RT\ln a_-^{\nu_-} = RT\ln a_+^{*\nu_+} + RT\ln a_-^{*\nu_-}$$

- Therefore we can write:

Eqn 32
$$a_+^{\nu+}a_-^{\nu-} = a_+^{*\nu+}a_-^{*\nu-}$$

- Assuming dilute solutions where the activities are approximately equal to the concentrations:

Eqn 33
$$\left(\frac{c_+}{c_+^*}\right)^{\nu+} = \left(\frac{c_-^*}{c_-}\right)^{\nu-}$$

Eqn 34
$$\left(\frac{\nu_+ c_s}{\nu_+ c_s^*}\right)^{\nu+} = \left(\frac{\nu_- c_s^*}{\nu_- c_s + \frac{ic_2}{\nu_- z_-}}\right)^{\nu-}$$

Eqn 35
$$\left(\frac{c_s}{c_s^*}\right)^{\nu+} = \left(\frac{c_s^*}{c_s + \frac{ic_2}{\nu_- z_-}}\right)^{\nu-}$$

Eqn 36
$$\frac{c_s^* - c_s}{c_s^*} = 1 - \left(\frac{c_s^*}{c_s + \frac{ic_2}{\nu_- z_-}}\right)^{\frac{\nu-}{\nu+}} = 1 - \frac{c_s^*}{c_s + \frac{ic_2}{\nu_- z_-}} = \frac{ic_2}{\hat{\nu} z_- c_s^*} - \left(\frac{1}{2 z_+ z_- \hat{\nu}^2}\right)\left(\frac{ic_2}{c_s^*}\right)^2$$

- Derivation of this equation in appendix

- Now Eqn 27 becomes:

Eqn 37
$$\left(\Delta\mu_1\right)_{ion}^* - \left(\Delta\mu_1\right)_{ion} = \nu_{m,1} RT\left(\frac{i^2 c_2^2}{2 z_+ z_- \hat{\nu} c_s^*}\right)$$

- But definition of ionic strength I is:

Eqn 38
$$I = \frac{1}{2}\sum_i^{all\_ions} z_i^2 c_i = \frac{z_+ z_- \hat{\nu} c_s^*}{2}$$ **…for a 1:1 electrolyte**

  - Where z_i is the charge on ion *i*

- Therefore:

Eqn 39
$$\left(\Delta\mu_1\right)_{ion}^* - \left(\Delta\mu_1\right)_{ion} = \nu_{m,1} RT\left(\frac{i^2 c_2^2}{4I}\right) = \nu_{m,1} RT\left(\frac{i^2 \phi_{2,s}^2}{4 I \nu_{sp,2}^2 M_0^2}\right)$$

- (Using relation $c_2 = \frac{\phi_{2,s}}{\nu_{sp,2} M_0}$ =moles ionizable groups/volume)

- Eqn 39 can be re-cast in terms of the solution pH:

Eqn 40
$$\left(\Delta\mu_1\right)_{ion}^* - \left(\Delta\mu_1\right)_{ion} = \frac{\nu_{m,1} RT}{4I}\left(\frac{K_a}{10^{-pH} + K_a}\right)^2\left(\frac{\phi_{2,s}}{z_- \nu_{sp,2} M_0}\right)^2 = \nu_{m,1} RT\left(\frac{K_a}{10^{-pH} + K_a}\right)^2\left(\frac{\phi_{2,s}^2}{4 I \nu_{sp,2}^2 M_0^2}\right)$$

- Returning to the equilibrium criterion:

Eqn 41

$$v_{m,1}\left(\frac{10^{-pK_a}}{10^{-pH}+10^{-pK_a}}\right)^2\left(\frac{\phi_{2,s}^2}{4Iv_{sp,2}^2M_0^2}\right)=\ln(1-\phi_{2,s})+\phi_{2,s}+\chi\phi_{2,s}^2+\phi_{2,r}\left(\frac{v_{m,1}}{v_{sp,2}M_c}\right)\left(1-\frac{2M_c}{M}\right)\left[\left(\frac{\phi_{2,s}}{\phi_{2,r}}\right)^{1/3}-\frac{1}{2}\left(\frac{\phi_{2,s}}{\phi_{2,r}}\right)\right]$$

- Brannon-Peppas paper analyzes Polyacrylates/polymethacrylates:
  - In water pH 7.0 with I = 0.35
  - χ = 0.8
  - pK_a = 6.0
  - $v_{sp,2}$ = 0.8 cm^3/g
  - M = 75,000 g/mole
  - M_c = 12,000 g/mole
  - M_0 = 90 g/mole
  - $\phi_{2,r}$ = 0.5

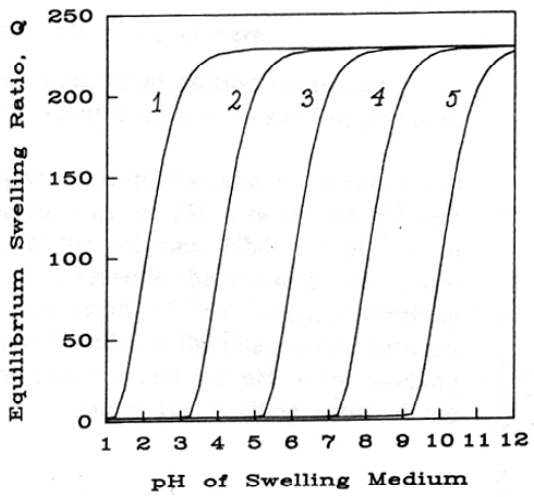

Fig. 3. Theoretical swelling predictions at comparable ionic strength conditions for an anionic network with: (1) $pK_a = 2.0$, (2) $pK_a = 4.0$, (3) $pK_a = 6.0$, (4) $pK_a = 8.0$, and (5) $pK_a = 10.0$.

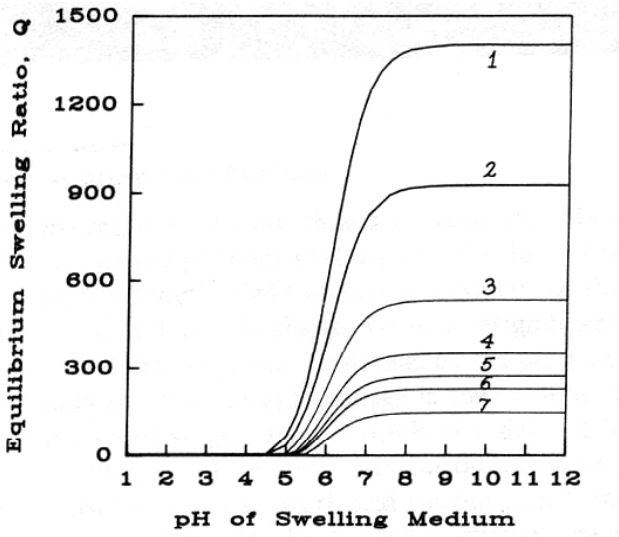

Fig. 4. Theoretical swelling predictions at comparable ionic strength conditions for an anionic network with: (1) $I = 0.05$, (2) $I = 0.1$, (3) $I = 0.25$, (4) $I = 0.5$, (5) $I = 0.75$, (6) $I = 1.0$, and (7) $I = 2.0$.

References

1. De, S. K. et al. Equilibrium swelling and kinetics of pH-responsive hydrogels: Models, experiments, and simulations. *Journal of Microelectromechanical Systems* **11**, 544-555 (2002).
2. Tanaka, T. & Fillmore, D. J. Kinetics of Swelling of Gels. *Journal of Chemical Physics* **70**, 1214-1218 (1979).
3. Zhao, B. & Moore, J. S. Fast pH- and ionic strength-responsive hydrogels in microchannels. *Langmuir* **17**, 4758-4763 (2001).
4. Chornet, E. & Dumitriu, S. Inclusion and release of proteins from polysaccharide-based polyion complexes. *Adv Drug Deliv Rev* **31**, 223-246. (1998).
5. Zhu, Y., Gao, C., He, T., Liu, X. & Shen, J. Layer-by-Layer assembly to modify poly(L-lactic acid) surface toward improving its cytocompatibility to human endothelial cells. *Biomacromol.* **4**, 446-452 (2003).
6. Khopade, A. J. & Caruso, F. Stepwise self-assembled poly(amidoamine) dendrimer and poly(styrenesulfonate) microcapsules as sustained delivery vehicles. *Biomacromolecules* **3**, 1154-1162 (2002).
7. Caruso, F., Trau, D., Mohwald, H. & Renneberg, R. Enzyme encapsulation in layer-by-layer engineered polymer multilayer capsules. *Langmuir* **16**, 1485-1488 (2000).
8. Elbert, D. L., Herbert, C. B. & Hubbell, J. A. Thin polymer layers formed by polyelectrolyte multilayer techniques on biological surfaces. *Langmuir* **15**, 5355-5362 (1999).
9. Wang, Y. F., Gao, J. Y. & Dubin, P. L. Protein separation via polyelectrolyte coacervation: Selectivity and efficiency. *Biotechnology Progress* **12**, 356-362 (1996).
10. Beebe, D. J. et al. Functional hydrogel structures for autonomous flow control inside microfluidic channels. *Nature* **404**, 588-+ (2000).
11. Beebe, D. J., Mensing, G. A. & Walker, G. M. Physics and applications of microfluidics in biology. *Annual Review of Biomedical Engineering* **4**, 261-286 (2002).
12. James, H. M. & Guth, E. Simple presentation of network theory of rubber, with a discussion of other theories. *J. Polym. Sci.* **4**, 153-182 (1949).
13. Flory, P. J. & Rehner Jr., J. Statistical mechanics of cross-linked polymer networks. I. Rubberlike elasticity. *J. Chem. Phys.* **11**, 512-520 (1943).
14. Flory, P. J. & Rehner Jr., J. Statistical mechanics of cross-linked polymer networks. II. Swelling. *J. Chem. Phys.* **11**, 521-526 (1943).
15. Brannonpeppas, L. & Peppas, N. A. Equilibrium Swelling Behavior of Ph-Sensitive Hydrogels. *Chemical Engineering Science* **46**, 715-722 (1991).
16. Peppas, N. A. & Merrill, E. W. Polyvinyl-Alcohol) Hydrogels - Reinforcement of Radiation-Crosslinked Networks by Crystallization. *Journal of Polymer Science Part a-Polymer Chemistry* **14**, 441-457 (1976).
17. Ozyurek, C., Caykara, T., Kantoglu, O. & Guven, O. Characterization of network structure of poly(N-vinyl 2-pyrrolidone/acrylic acid) polyelectrolyte hydrogels by swelling measurements. *Journal of Polymer Science Part B-Polymer Physics* **38**, 3309-3317 (2000).